10th Brazilian Congress on Manufacturing Engineering
August 05th-07th, 2019, São Carlos, SP, Brazil

AUSTENITIC STAINLESS STEEL SCRATCH TESTS: ABRASIVE MICRO-MECHANISMS AND HARD SECOND PHASE INFLUENCE

Vanessa Seriacopi
Federal Institute of Sao Paulo, Câmpus Guarulhos, Av. Salgado Filho, 3501 - Centro, Guarulhos - SP, 07115-000, Brazil.
Escola Politécnica of University of Sao Paulo, Surface Phenomena Laboratory, Av. Prof. Mello Moraes, 2231 – Cidade Universitária – SP, 05508-030, Brazil.
vanessa.seriacopi@gmail.com

Newton Kiyoshi Fukumasu
Izabel Fernanda Machado
Escola Politécnica of University of Sao Paulo, Surface Phenomena Laboratory, Av. Prof. Mello Moraes, 2231 – Cidade Universitária – SP, 05508-030, Brazil.
newton.fukumasu@usp.br, machadoi@usp.br

Abstract. *Abrasive mechanisms are present in many manufacturing processes, such as grinding, lapping, belt finishing and honing. These complex systems can be studied from a tribological point of view, in which the material removed, and coefficient of friction behaviors can help to evaluate the material requirements. Some simplified hypotheses can be adopted during this study to define the best conditions in service. In this sense, the aim of this work is to analyze the abrasion influence onto a heterogeneous austenitic stainless steel using micro-scratch tests. This work contributes to provide the microstructure importance in terms of material design, especially applied to abrasive manufacturing processes. The proposal is to conduct a numerical-experimental approach, focusing on verifying the hard second phase particle effects. The normal load was constant during the tests, within a range from 40 to 100 mN. The abrasive particle was simplified, based on a cono-spherical geometry with 10 μm tip diameter and 60° apex angle. Finite Element Analyses were carried out using the TriboCODE coupled to Abaqus®/Explicit module. As conclusions, the hard second phase particles led to a reduction of the depth of penetration, wear track width and material removal, when compared to the soft austenitic matrix of the material.*

Keywords: *abrasive mechanisms, micro-scratch tests, normal load, numerical-experimental approach, microstructure.*

1. INTRODUCTION

Manufacturing processes with undefined tool edge geometry (e.g. grinding, polishing and honing) can result in different abrasive mechanisms, ranging from ploughing to cutting. The ploughing mechanism consists of plastic deformation, while the cutting mechanism promotes a considerable material removal due to the severity of plastic deformation of the material (Hokkirigawa and Kato 1988; Hokkirigawa, Kato, and Li 1988; Gahr 1987; Hutchings and Shipway 2017).

Focusing on the abrasion due to a single scratching, according Franco (2015), Seriacopi et al. (2016) and Seriacopi (2017), unique abrasive mechanisms were not observed in the wear track throughout micro-scratch tests onto cast iron, tool steels and austenitic stainless steels; however, a prevailing mechanism was verified in each case of normal load applied. This fact indicated that the transition from ploughing to cutting could not be considered sudden.

Additionally, computational simulations have been used to better understand the microstructural influence on the scratch test and, therefore, related the abrasion aspects. Relationships between the morphology of the second phase particles and abrasive shapes, as well as the volume fraction and distribution of the second phase were investigated, using Micro-Scale Dynamic Model (MSDM), by Hu, Li, and Llewellyn (2007). Tkaya et al. (2009) evaluated, using Finite Element Method (FEM), the influence of the graphite features on the plastic deformation and subsurface crack formation in a nodular cast iron. More recently, some findings about the influence of the mechanical properties of the second phase during the scratch tests were reported (Pöhl et al. 2015; Pöhl, Mohr, and Theisen 2017). Using FEM and constant normal load, the authors observed that spherical precipitates significantly smaller than the wear track width, even hard, did not increase the abrasion resistance. These simplified precipitates were removed, occurring chip formation. In turn, hard and greater precipitates lead to a reduction of the local penetration depth and width, increasing the abrasion resistance of the material.

Even though, in the majority of the cases, the analyses of the abrasive manufacturing processes were carried on the homogeneous materials. Microstructure features, such as morphology, size and distribution of the second phase, were mainly disregarded, specifically in the experimental coupled with computational field, due to the complexity of these issues.

In this context, the objective of this work consists of studying the effect of a hard second phase particle (TiN) in the AISI 310 stainless steel matrix during micro-scratch tests. The developed procedure intends to reinforce the concept of the microstructure importance on the mechanical, failure and tribological behaviors. Also, a range of normal load is considered to evaluate the abrasive mechanisms (mild and severe abrasion). To reach this aim, numerical simulations using FEM and experimental tests are conducted, providing outcomes in terms of: depth of penetration, apparent coefficient of friction and removed volume.

2. MATERIALS AND METHODS

The studied material was the AISI 310 austenitic stainless steel, whose microstructure can be observed in Fig.1a. First of all, to simplify the approach, the grain and the twins were not taken into account in the modelling. Concerning the scratch tests, two regions of this material were separated for the analyses: (a) an austenitic matrix, as-annealed, with mechanical properties similar to the AISI 304 steel in these conditions; and (b) second phase particles of TiN, which were six times harder than the matrix.

The computational methodology of this work was developed using the TRIBOCode digital tribology package in development at the "Laboratório de Fenômenos de Superfície" (LFS) of the University of Sao Paulo, Brazil (Fukumasu et al. 2018). This package is based on several modules, used to analyze multi-scale tribological phenomena presenting complex material microstructural and physical mechanisms, such as abrasion, adhesion and thermal/contact fatigue. In this work, the abrasion module was used to analyze micro-scratch tests of the heterogeneous materials.

Geometry: To obtain the morphology and size of the second phase particles, a tomography of the slab material was carried out, using a 3D X-ray microscope XRadia VersaXRM-510 by Zeiss®. After the image treatment (Seriacopi 2017), the microstructure was imported in the Abaqus® software/Explicit module, and a mesh was assigned to this region (Fig.1c) with the features as follows: domain of 228 x 85 x 33 µm³, discretized by 3,143,252 linear hexahedral elements of the C3D8 type. Furthermore, the abrasive particle was represented by a cono-spherical geometry, with 5 µm tip radius and 60° apex angle, to reproduce the experimental apparatus (Fig.1b). In the modelling, the abrasive was considered as an analytical-rigid part.

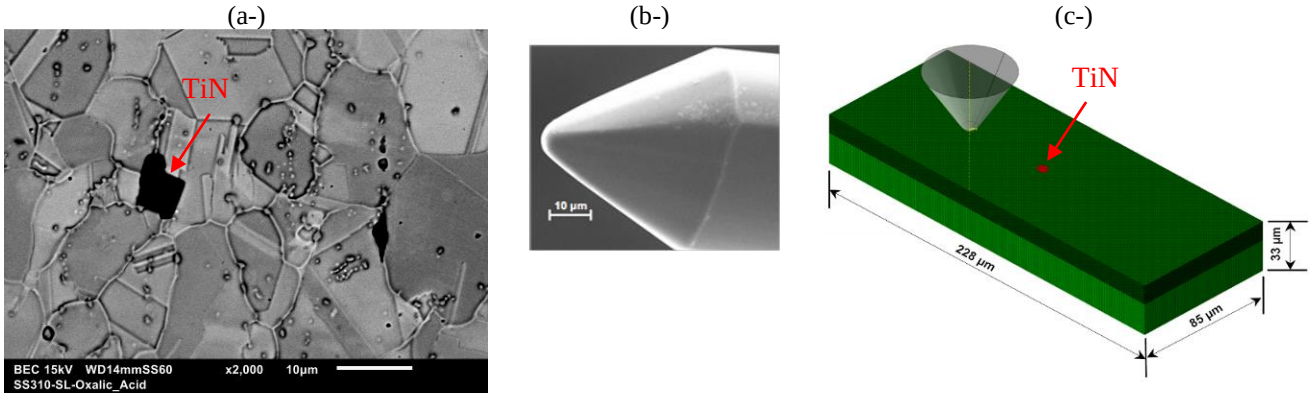

Figure 1. (a-) AISI 310 steel microstructure (etching: oxalic acid): SEM image – backscattering electrons; (b-) diamond tip with cono-spherical geometry used in the tests; (c-) 3D mesh used in the FEM modelling of micro-scratch tests: austenitic matrix (in green) and TiN (in red).

Mechanical Properties: Throughout the numerical simulation by FEM, the matrix material was considered elastic-plastic. Likewise, the precipitate material was elastic. Their properties can be seen in Tab.1; these data were experimentally measured (tensile and instrumented indentation tests) and listed in the literature.

Table 1. Mechanical properties applied to model the scratch tests of the AISI 310 steel slab.

Phase	Density (kgm^{-3})	Elastic Modulus (GPa)	Poisson Ratio	Elongation - ε_{total} (%)	Yield Stress - σ_y (MPa)	Ultimate Strength – UTS (MPa)	Hardness (GPa)	Reference
Austenitic matrix (AISI 304 steel) - annealed bar (longitudinal)	8,000	212	0.29	60	235	585	2.47	(ASM International. 1990; Seriacopi 2017)
TiN	5,400	106	0.25	-	-	-	15.5	(Pierson 1996; Seriacopi 2017)

Damage Properties: The Ductile Model was assigned to the austenitic matrix, whereas the Brittle Model was used to specify the damage behavior of the TiN particles. Combined with the element deletion, both models were applied to simulate the material removal when a critical condition was achieved. Regarding the ductile model, the damage nucleation of the austenitic matrix was provided by the curve of the fracture strain as a function of the stress triaxiality, obtained from the literature (adapted from Dzugan et al. 2012; Kim et al. 2013). In turn, the triaxiality is defined as the negative ratio between the hydrostatic pressure and von Mises equivalent stress (Bao and Wierzbicki 2004). In this work, the triaxiality was specified between -0.13 and 3.0 corresponding to a fracture strain range between 1.4 and 0.1. The ductile damage evolution was given by the critical energy release rate G_f = 0.375 Nmm^{-1}, as discussed in Seriacopi (2017). Additionally, Tab.2 displays the parameters used to model the brittle damage of the TiN second phase particles.

Table 2. Based on the literature, properties assigned to the brittle damage model – TiN second phase particles.

Phase	Fracture toughness (MPa $m^{1/2}$)	Critical energy release rate - (Nmm^{-1})	Failure stress - (GPa)	Failure strain	Reference
TiN	2.5	0.022	5.17	0.019	(Demirskyi, Agrawal, and Ragulya 2013)

Loading Conditions: Normal load was imposed as constant during the scratch test. Based on Hokkirigawa, Kato, and Li (1988) and Seriacopi et al. (2016), the range from 40 to 100 mN was considered in the analyses to investigate the abrasive mechanisms using the numerical approach. In this case, the scratch length corresponded to 100 μm.

Moreover, experimental tests were conducted to validate the computational modelling. Focusing on the experimental step, specimens of the AISI 310 austenitic stainless steel, as-annealed, were obtained from the longitudinal section of bars. The procedure for the metallographic sample preparation is found in literature (Seriacopi 2017). After the mechanical polishing, these specimens were submitted to the single-pass scratch tests, using a diamond indenter with the same geometry used in the model. Experimental tests were conducted in the TI-950 triboindenter from Bruker Inc., applying its high load module (until 2 N) and acquiring the force and displacement signals in the 3D Cartesian system. Table 3 depicts the parameters utilized for the experimental scratch tests, which followed the recommendations found in ASTM Standard G171 – 03 (American Society for Testing and Materials 2009). Afterwards, abrasive mechanisms of the specimens were characterized by Scanning Electron Microscope (SEM), JSM Jeol 6010LA.

Table 3. Experimental parameters of the scratch tests to allow a suitable comparison with the numerical results.

Normal Loads (mN)	Scratch Length (μm)	Scratching Velocity (μm s^{-1})	Data Acquisition Rate (Hz)
40, 50, 60, 70, 80 and 100	60	10	200

3. RESULTS AND DISCUSSIONS

As shown in Tab.4, regarding the penetration depth and material removal, the differences between numerical and experimental results were up to 10%. This indicate a well calibrated numerical model, in which such uncertainty level can be related to the mesh discretization limit and material local properties. Conversely, for the austenitic stainless steels, the higher work-hardening has a significant influence on the material response during scratch tests, which leads to an overall variation of the penetration depth. Focusing on the numerical results, the depth of penetration increased linearly with the normal load, providing a good linear correlation coefficient (R^2 = 0.83). This relation was also observed for other steel classes by Franco (2015) and Trzepieciński et al. (2015).

Table 4. Comparison between numerical and experimental results, and their differences, in view of the following outputs: (i) depth of penetration; (ii) apparent coefficient of friction (tangential force / normal force); and (iii) removed volume, which was calculated based on the depth of penetration.

Normal Load (mN)	Depth of penetration (μm)			Apparent Coefficient of Friction (COF)			Removed Volume ($\mu m^3/\mu m$)		
	Numerical	Experimental	Difference (%)	Numerical	Experimental	Difference (%)	Numerical	Experimental	Difference (%)
40	0.47	0.45	↑ 4.4	0.15	0.18	↓ 17	1.3	1.2	↑ 8.3
50	0.55	0.55	0	0.24	0.21	↓ 14	1.7	1.7	0
60	0.86	0.80	↑ 7.5	0.30	0.28	↓ 7.1	3.3	3.0	↑ 10
70	1.19	1.14	↑ 4.4	0.43	0.48	↓ 10	5.3	5.0	↑ 6.0
80	1.36	1.34	↑ 1.5	0.58	0.58	0	6.4	6.3	↑ 1.6
100	2.07	2.02	↑ 2.5	0.78	0.76	↑ 2.6	11.7	11.3	↑ 3.5

Furthermore, apparent COF from numerical results produced considerable differences when compared with the experimental values (Tab.4), especially for the lower normal loads. From 40 to 70 mN, numerical COF values were

smaller than the experimental values. This fact seems to be a consequence of the numerical model did not consider the adhesion parcel effect on the coefficient of friction. For this reason, Tab.4 shows that these numerical and experimental differences were reduced from 80 to 100 mN, in which a severe micro-cutting can be characterized (Seriacopi 2017); i.e. the abrasion prevails over the adhesion.

Figure 2a shows the wear track, resulting from the numerical simulation of the scratch tests in micro-scale. In general, the load-based dominant abrasive mechanism can be observed: micro-ploughing (mild abrasion) for 40 mN; transition from micro-ploughing to micro-cutting for 50 mN; a less severe micro-cutting for 60 mN; and a more severe micro-cutting for 80 mN. The scratch width tends to decrease when the abrasive crosses the hard second phase particle (TiN), which suggests a local reduction of the material removal. In fact, the experimental results (Fig.2b) corroborate that the removed volume is lower in the TiN region when compared to the matrix region. Moreover, the rigid abrasive can have a high resistance to proceed its path over the TiN and, for the higher loads (e.g. 80 mN), a local brittle failure mode may be verified (Fig.2a). Thus, an increase of the specific cutting energy can be predicted (Seriacopi 2017). As expected due to the wear behavior, the depth of penetration is also reduced in this region (Fig.2b).

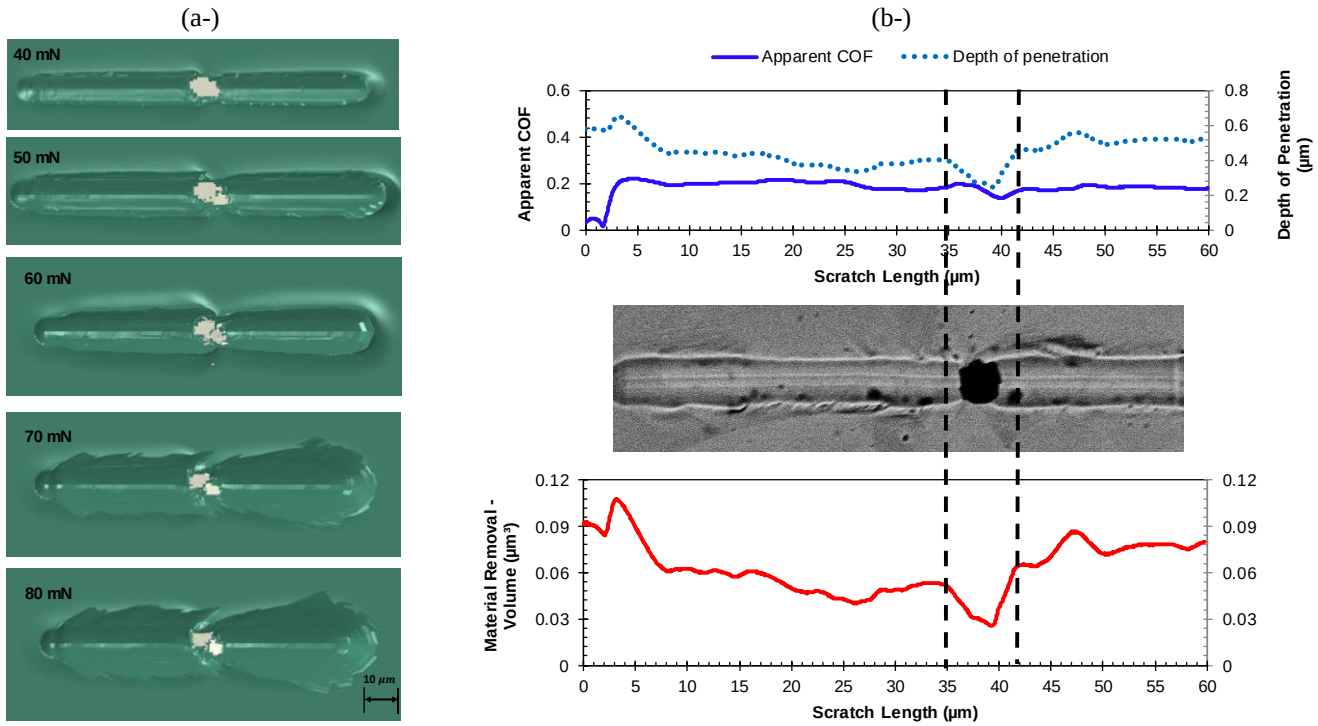

Figure 2. (a-) Numerical results of the scratch tests onto the austenitic matrix (in green) and TiN (in white) – top view; (b-) experimental results for the 40 mN normal load condition, with local effects highlighted.

The apparent coefficient of friction decreased when the abrasive tip passes over the TiN (Fig.2b), since the hard second phase plays an important role in terms of the system energy variations A great part of the energy is spent due to the severe plastic deformation of the austenitic matrix throughout the scratch tests. On the other hand, in the TiN region, only contributions of the elastic deformation and a possible fracture can affect the energy balance (Moore 1979). Consequently, a local reduction of the dissipated energy and apparent COF was promoted from the ductile matrix to the brittle second phase particle.

4. CONCLUDING REMARKS

In conclusion, the results of this work emphasize the importance of the study focused on the microstructure in the tribosystems. Albeit fundamental, the present numerical-experimental approach is relevant to show that a hard second phase affects the tribological behavior of the material when submitted to an abrasive process by using micro-scratch tests. In addition, the mechanical and damage properties of the phases contained in a stainless steel were deterministic in the analyses. Some aspects of this work could be highlighted:

- The numerical model was validated by experimental tests: In terms of average removed volume (and depth of penetration), the numerical results are in accordance with the experimental results with an error up to 10%;
- The hard and brittle second phase particle resulted in a local reduction of the penetration depth, removed volume and apparent friction coefficient. The analyses in terms of system energies lead to understand these effects;

- The prevailing abrasive micro-mechanisms were investigated with respect the normal load range, from micro-ploughing to micro-cutting. The excessive plastic deformation of the austenitic matrix as well as the brittle failure of the second phase particles can contribute to the material removal by cutting.

Finally, this prior evaluation pointed out that the design of the materials should be investigated taking into account the microstructural aspects, to improve the understanding about their responses throughout the manufacturing process applications.

5. ACKNOWLEDGEMENTS

This work was conducted during a Ph.D. scholarship supported by the National Council for Scientific and Technological Development (CNPq) at the University of Sao Paulo (Process Number: 162001/2013-4). The authors are very grateful to CNPq and FAPESP for the financial support.

6. REFERENCES

American Society for Testing and Materials. 2009. *ASTM G171 - 03(2009)E2: Standard Test Method for Scratch Hardness of Materials Using a Diamond Stylus*. *ASTM International*. West Conshohocken, PA (USA): ASTM International.

ASM International. 1990. *ASM Handbook, Volume 1: Properties and Selection: Irons, Steels, and High-Performance Alloys*. ASM Handbook. USA: ASM International.

Bao, Yingbin, and Tomasz Wierzbicki. 2004. "On Fracture Locus in the Equivalent Strain and Stress Triaxiality Space." *International Journal of Mechanical Sciences* 46 (1): 81–98.

Demirskyi, D., D. Agrawal, and A. Ragulya. 2013. "Comparisons of Grain Size-Density Trajectory during Microwave and Conventional Sintering of Titanium Nitride." *Journal of Alloys and Compounds* 581: 498–501.

Dzugan, J, M Spaniel, P Konopík, J Ruzicka, and J Kuzelka. 2012. "Identification of Ductile Damage Parameters for Austenitic Steel." *World Academy of Science, Engineering and Technology* 6 (5): 1291–96.

Franco, Luiz Alberto Pereira das Neves. 2015. "Abrasion of Gray Cast Iron: Application to Automotive Engines." PhD Thesis - Univeristy of Sao Paulo (In portuguese).

Fukumasu, N. K., C. F. Bernardes, M. A. Ramirez, V. J. Trava-Airoldi, R. M. Souza, and I. F. Machado. 2018. "Local Transformation of Amorphous Hydrogenated Carbon Coating Induced by High Contact Pressure." *Tribology International* 124 (December 2017): 200–208.

Gahr, Karl-Heinz Zum. 1987. "Microstructure and Wear of Materials." *Tribology Series* 10.

Hokkirigawa, K., and K. Kato. 1988. "An Experimental and Theoretical Investigation of Ploughing, Cutting and Wedge Formation during Abrasive Wear." *Tribology International* 21 (1): 51–57.

Hokkirigawa, K., K. Kato, and Z. Z. Li. 1988. "The Effect of Hardness on the Transition of the Abrasive Wear Mechanism of Steels." *Wear* 123 (2): 241–51.

Hu, J, D Y Li, and R Llewellyn. 2007. "Synergistic Effects of Microstructure and Abrasion Condition on Abrasive Wear of Composites — A Modeling Study" 263: 218–27.

Hutchings, Ian, and Philip Shipway. 2017. *Tribology: Friction and Wear of Engineering Materials*. 2nd ed. UK: Butterworth-Heinemann.

Kim, J-H., N-H. Kim, Y-J. Kim, K Hasegawa, and K Miyazaki. 2013. "Ductile Fracture Simulation of 304 Stainless Steel Pipes with Two Circumferential Surface Cracks." *Fatigue & Fracture of Engineering Materials & Structures* 36 (10): 1067–80.

Moore, M. 1979. "Energy Dissipation in Abrasive Wear." *Conference on Wear of Materials*, 636–38.

Pierson, Hugh O. 1996. "11 - Interstitial Nitrides: Properties and General Characteristics BT - Handbook of Refractory Carbides and Nitrides." In *Handbook of Refractory Carbides & Nitrides: Properties, Characteristics, Processing and Applications*, 181–208. Westwood, NJ: William Andrew Publishing.

Pöhl, F., A. Mohr, and W. Theisen. 2017. "Effect of Matrix and Hard Phase Properties on the Scratch and Compound Behavior of Wear Resistant Metallic Materials Containing Coarse Hard Phases." *Wear* 376–377: 947–57.

Pöhl, F., S. Schwarz, P. Junker, K. Hackl, and W. Theisen. 2015. "Indentation and Scratch Testing – Experiment and Simulation." *International Conference on Stone and Concrete Machining (ICSCM)* 3 (0): 292–308.

Seriacopi, V. 2017. "Evaluation of Abrasive Mechanisms in Metallic Alloys during Scratch Tests: A Numerical-Experimental Study in Micro-Scale." PhD Thesis - Univeristy of Sao Paulo.

Seriacopi, V, N K Fukumasu, R M Souza, and I F Machado. 2016. "Analysis of Abrasion Mechanisms in the AISI 303 Stainless Steel: Effect of Deformed Layer." *Procedia CIRP* 45: 187–90.

Tkaya, M. B., S. Mezlini, M. El Mansori, and H. Zahouani. 2009. "On Some Tribological Effects of Graphite Nodules in Wear Mechanism of SG Cast Iron: Finite Element and Experimental Analysis." *Wear* 267 (1–4): 535–39.

Trzepieciński, Tomasz, Łukasz Bąk, Feliks Stachowicz, Sergei Bosiakov, and Sergei Rogosin. 2015. "Analysis of Contact of a Rigid Sphere against a Deformable Flat." *Acta Metallurgica Slovaca* 21 (4): 285–92.

7. RESPONSIBILITY NOTICE

The authors are the only responsible for the printed material included in this paper.